

Crystal structures of oxidized and reduced mitochondrial thioredoxin reductase provide molecular details of the reaction mechanism

Ekaterina I. Biterova, Anton A. Turanov, Vadim N. Gladyshev, and Joseph J. Barycki[†]

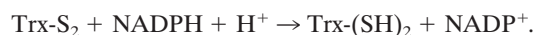
Department of Biochemistry, University of Nebraska, Lincoln, NE 68588-0664

Edited by Martha L. Ludwig, University of Michigan, Ann Arbor, MI, and approved September 4, 2005 (received for review May 20, 2005)

Thioredoxin reductase (TrxR) is an essential enzyme required for the efficient maintenance of the cellular redox homeostasis, particularly in cancer cells that are sensitive to reactive oxygen species. In mammals, distinct isozymes function in the cytosol and mitochondria. Through an intricate mechanism, these enzymes transfer reducing equivalents from NADPH to bound FAD and subsequently to an active-site disulfide. In mammalian TrxRs, the dithiol then reduces a mobile C-terminal selenocysteine-containing tetrapeptide of the opposing subunit of the dimer. Once activated, the C-terminal redox center reduces a disulfide bond within thioredoxin. In this report, we present the structural data on a mitochondrial TrxR, TrxR2 (also known as TR3 and TxnRd2). Mouse TrxR2, in which the essential selenocysteine residue had been replaced with cysteine, was isolated as a FAD-containing holoenzyme and crystallized (2.6 Å; $R = 22.2\%$; $R_{\text{free}} = 27.6\%$). The addition of NADPH to the TrxR2 crystals resulted in a color change, indicating reduction of the active-site disulfide and formation of a species presumed to be the flavin-thiolate charge transfer complex. Examination of the NADP(H)-bound model (3.0 Å; $R = 24.1\%$; $R_{\text{free}} = 31.2\%$) indicates that an active-site tyrosine residue must rotate from its initial position to stack against the nicotinamide ring of NADPH, which is juxtaposed to the isoalloxazine ring of FAD to facilitate hydride transfer. Detailed analysis of the structural data in conjunction with a model of the unusual C-terminal selenenylsulfide suggests molecular details of the reaction mechanism and highlights evolutionary adaptations among reductases.

disulfide | flavoprotein | selenocysteine | selenoprotein

Thioredoxins are the major cellular protein disulfide reductases and are responsible for the regulation of numerous biochemical processes within the cell (1). These proteins are maintained in a reduced state by thioredoxin reductases (TrxR), homodimeric flavoproteins that catalyze the NADPH-dependent reduction of thioredoxins (2, 3).



Two forms of TrxRs have evolved with related but distinct modes of catalysis (2–5). Low- M_r TrxRs ($M_r \approx 35$ kDa) are typically found in prokaryotes, archaea, plants, and lower eukaryotes, whereas high- M_r TrxRs ($M_r \approx 55$ kDa) are observed in higher eukaryotes. To date, only the green alga *Chlamydomonas reinhardtii* has been shown to contain both a low- and a high- M_r TrxR (6).

The general features of catalysis are retained in both low- and high- M_r TrxR (2, 4). TrxR transfers reducing equivalents from NADPH to its bound FAD, ultimately leading to the reduction of an active-site disulfide. In low- M_r TrxRs, the catalytic cycle requires a large conformational change after dithiol activation (4, 7, 8). In high- M_r TrxR, the active-site dithiol reduces a third redox active center in the highly mobile C terminus of the opposing subunit. This third group is responsible for the reduction of the disulfide bond within thioredoxin. Its nature is species-specific and ranges from a C-X-X-X-X-C disulfide in

Plasmodium falciparum (9) to a vicinal disulfide in *Drosophila melanogaster* (10) or a vicinal selenenylsulfide in mammalian TrxRs (11, 12).

In mammalian systems, three isozymes of high- M_r TrxRs have been identified: a cytosolic (TrxR1) (11, 12), a mitochondrial (TrxR2) (13), and an isozyme highly expressed in testes (14, 15). Targeted disruption of either TrxR1 (16) or TrxR2 (17) genes results in an embryonic lethal phenotype, and TrxR1 and TrxR2 appear to have nonredundant functions (16–19). TrxR1 null embryos are affected primarily by compromised cell proliferation (16), whereas TrxR2 null embryos suffer from severe anemia and improper heart development (17). Splice variants of TrxR1 and TrxR2 have also been identified, including a variant that would result in the targeting of TrxR2 to the cytosol (20–24). However, the biological implications of these variations have not been resolved and would benefit from additional biochemical and structural characterizations of the enzymes.

Numerous biochemical and computational studies have added to our understanding of the catalytic mechanism of high- M_r TrxR (2–5, 15, 25–28). Reduction of the enzyme by a single equivalent of NADPH leads to several two-electron reduced species (EH₂), with a thiolate-flavin charge transfer complex predominating. Addition of a second equivalent of NADPH leads to a four-electron reduced enzyme (EH₄) in which both the active-site disulfide and the selenosulfide-containing C-terminal tail of the opposing subunit are likely reduced. Once reduced to the EH₄ state, the enzyme catalyzes a disulfide exchange between the activated C-terminal tail and oxidized thioredoxin. To date, the molecular details of selenenylsulfide/disulfide exchange have not been determined.

Recently, the first x-ray structure of a high- M_r TrxR, rat cytosolic TrxR1, was described (29). The overall topology of this enzyme is similar to that of other pyridine nucleotide disulfide oxidoreductases, particularly glutathione reductases (30–35), and is in agreement with earlier modeling studies of high- M_r TrxRs (15). Interestingly, all of the residues in glutathione reductase responsible for substrate recognition are structurally conserved in rTrxR1, even though rTrxR1 cannot directly reduce oxidized glutathione. The authors (15) suggested that the mobile selenenylsulfide containing a C-terminal tail not only serves as a third redox active group, but it also blocks oxidized glutathione from binding to the enzyme. In addition, the structure confirmed the obligatory “head-to-tail” arrangement of high- M_r TrxR, with the redox-active C-terminal tail of one subunit interacting with the active site of the opposing subunit (36, 37). Unfortunately, the observed conformation of the C-terminal tail precluded direct interaction with the active-site disulfide/dithiol

This paper was submitted directly (Track II) to the PNAS office.

Abbreviation: TrxR, thioredoxin reductase.

Data deposition: The atomic coordinates have been deposited in the Protein Data Bank (PDB ID codes 1ZKQ and 1ZDL).

[†]To whom correspondence should be addressed. E-mail: jbarycki2@unl.edu.

© 2005 by The National Academy of Sciences of the USA

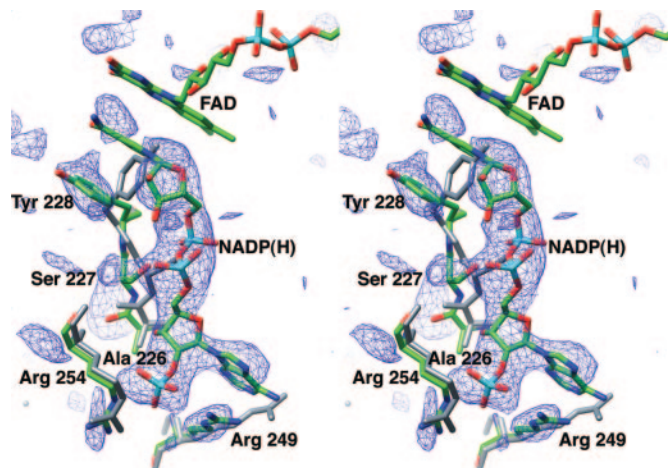


Fig. 3. Difference Fourier electron density map of the NADP(H)-binding site. Shown in the stereodiameter is the difference map contoured at $\approx 3\sigma$, superimposed with the final mTrxR2-NADP(H) model. Carbon atoms are colored in green, nitrogen atoms in blue, oxygen atoms in red, and phosphorous atoms in cyan. For comparison, the final model of the mTrxR2 holoenzyme is also shown (light blue).

correspond to more divergent regions of high- M_r TrxR primary structure. To reduce the bias introduced by a direct comparison of the mTrxR2 holoenzyme and mTrxR2-NADP(H) models, a difference Fourier electron density map was calculated by using the phases from the mTrxR2 holoenzyme. This $F_o - F_c$ map was used to assess the structural changes in mTrxR2 on addition of NADPH (Fig. 3). Continuous electron density was observed for the NADP(H) cofactor, although the quality of the map in the region of the nicotinamide ring was somewhat degraded by the placement of Tyr-228 in the oxidized mTrxR2 model. The positions of the isoalloxazine rings from each complex were nearly identical, and both ring systems were essentially planar.

Several significant displacements are observed in the mTrxR2-NADP(H) protein structure. Two arginine residues, Arg-249 and Arg-254, reorient to interact with the 2'-phosphate group of NADPH and likely confer the enzyme's specificity for NADPH relative to NADH (29). In addition, the hydroxyl group of Ser-227 must adjust to allow binding of one of the bridging phosphate groups of NADPH. Last, the $F_o - F_c$ map indicates that the side chain of Tyr-228 must rotate to accommodate NADPH. Thus, to orchestrate this critical catalytic event, Tyr-228, which normally shields the flavin ring of FAD from solvent in the absence of NADPH, must reposition itself to stack against the nicotinamide ring upon cofactor binding. A conserved tyrosine residue in human glutathione reductase, Tyr-197, has been shown to serve a comparable function (34, 45-47).

The importance of such a rotation of the conserved tyrosine residue upon pyridine nucleotide binding is illustrated by examination of the rTrxR1 structure (29). Density is not observed for the nicotinamide ring of NADP⁺ in the oxidized rTrxR1-NADP⁺ complex. The equivalent tyrosine residue, Tyr-200, is arranged to shield the flavin ring from solvent (Fig. 4A, blue model) and thus precludes efficient binding of NADP⁺. Only the adenosine portions of each cofactor have similar orientations in the rTrxR1 and mTrxR2 structures. The bridging phosphate groups and the nicotinamide ribose of rTrxR1-bound NADP⁺ are displaced significantly relative to the corresponding atoms in the mTrxR2-NADP(H) structure. Without reorientation of the conserved tyrosine residue, the nicotinamide and isoalloxazine rings cannot stack in the position necessary for hydride transfer.

Active Site of mTrxR2. The overall architecture of the mTrxR2 active site is comparable to that of rTrxR1 (Fig. 4B) (29) and

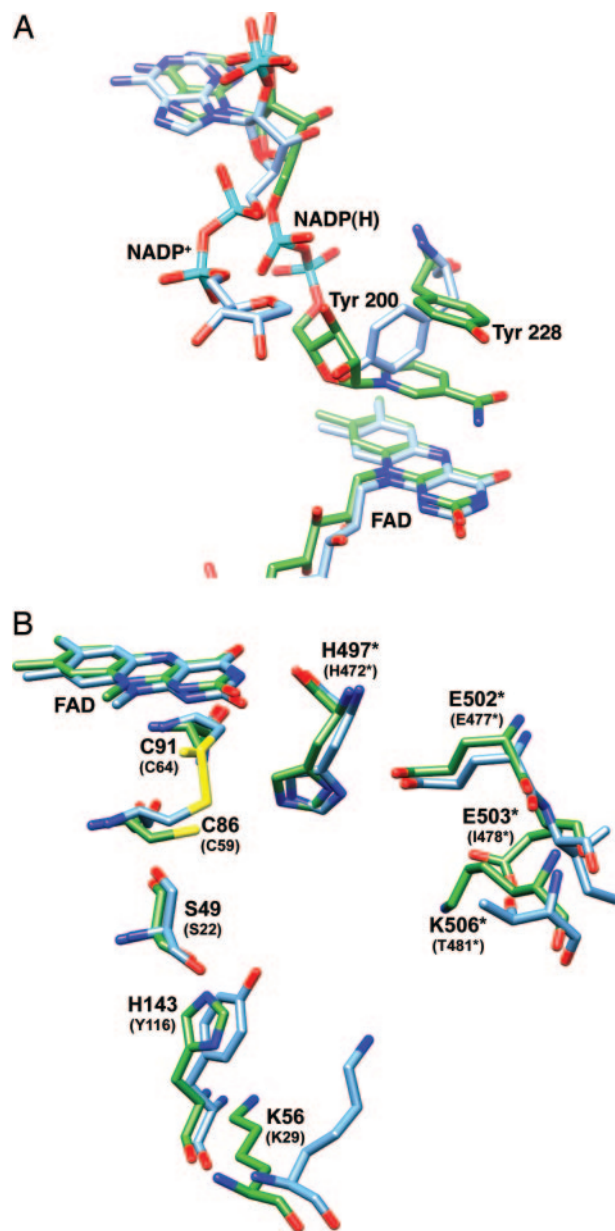


Fig. 4. Comparison of the active sites of mTrxR2 and rTrxR1. Models of mTrxR2 and rTrxR1 were superimposed and are shown as stick representations by using the color scheme described in Fig. 3. (A) NADP(H)-binding site. In mTrxR2 (green), the nicotinamide ring of NADP(H) is stacked above the isoalloxazine ring of FAD, but it is not observed in rTrxR1 (blue), because its binding site is occupied by the side chain of Tyr-200. (B) Region adjacent to the active-site disulfide/dithiol pair. Amino acid side chains of mTrxR2 are labeled with the corresponding residues from rTrxR1 given in parentheses. An asterisk denotes an amino acid residue from the opposing subunit of the dimer. Please note that, for FAD, only the isoalloxazine ring is presented. Thr-368 of mTrxR2 and Thr-339 of rTrxR1 adopt nearly identical conformation and have been omitted for clarity.

human glutathione reductase (31, 34, 46). In the mTrxR2-NADP(H) complex, the active-site disulfide/dithiol pair is observed in the reduced state, whereas this active-site redox center is found in the oxidized state in both the mTrxR2 holoenzyme (Fig. 1) and the rTrxR1-NADP⁺ complex (Fig. 4B). In addition to the active-site disulfide/dithiol functional group, a histidine-glutamate pair is located in similar orientations in these enzymes (H497*-E502* in mTrxR2; an asterisk designates an amino acid

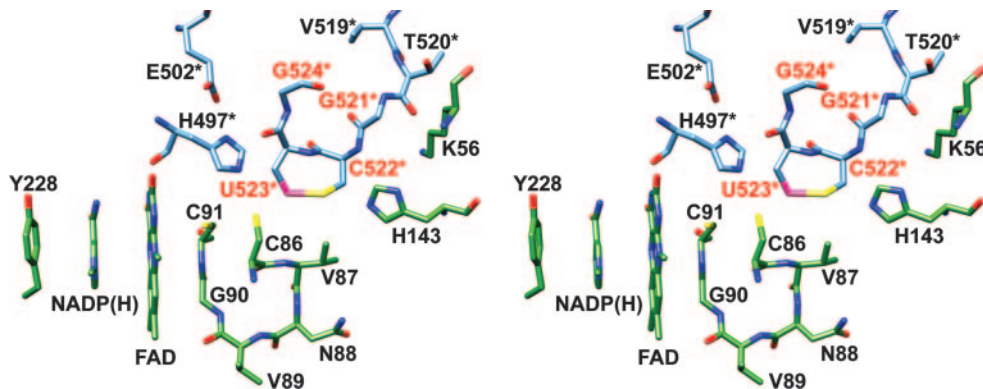


Fig. 5. Model of the C terminus of mTrxR2. Continuous density was not observed for the final four residues of the mTrxR2–NADP(H) structure, confirming its highly mobile nature. Thus, residues G521, C522, U523, and G524 were modeled into the active site. In the stereodiametric, the selenium atom is colored in pink, nitrogen atoms in blue, oxygen atoms in red, and sulfur atoms in yellow. Carbon atoms from subunit A are colored in green, and those from subunit B are in blue and are designated with asterisks. Modeled residues are labeled in red. For clarity, only the nicotinamide ring of NADP(H) and the isoalloxazine ring of FAD are presented.

from the opposing subunit). Mutagenesis studies have demonstrated that both cysteine residues, as well as the active-site histidine residue, are essential for efficient catalysis (27). Other functional groups of mTrxR2 that face into the enzyme active site include Lys-56, His-143, Glu-503*, and Lys-506*. Glu-503* and Lys-506* are positioned to form a salt bridge and may stabilize the placement of Glu-502*. Such an interaction is absent in human glutathione reductase and rTrxR1, but other hydrogen bond networks maintain the tertiary structure in this region. The epsilon amino group of Lys-56 is located ≈ 3.1 Å from ND1 of His-143 and may help position the imidazole ring. Interestingly, a tyrosine residue replaces His-143 in both human glutathione reductase (Tyr-114) and rTrxR1 (Tyr-116; Fig. 4B). This tyrosine residue has been implicated in catalysis (47), as discussed below, and thus substitution with a histidine residue may modulate the catalytic activity of mTrxR2 relative to these homologues.

Modeling of the Redox-Active C-Terminal Tail. The molecular details of how reducing equivalents are transferred from the disulfide/dithiol pair deep within the active site, to the mobile C-terminal tail containing the Gly-Cys-Sec-Gly motif, and ultimately to oxidized thioredoxin remain unresolved. In the structure of the rat cytosolic isozyme (29), the C terminus was arranged in such a conformation that the selenocysteine residue could not interact with the active-site disulfide/dithiol, suggesting that an alternate conformation for the C terminus must exist. In the current study, the C-terminal tail of mTrxR2 exhibits considerable conformational flexibility, as evidenced by the high B factors of its residues. Furthermore, the last four residues are not observed in the electron density.

The Gly-Cys-Sec-Gly motif of the mTrxR2–NADP(H) structure has been modeled into the active site of the enzyme (Fig. 5). A suitable template for the selenenylsulfide was identified, and the C terminus of the enzyme was positioned in the active site of the opposing subunit, optimizing interactions and minimizing geometric strains. Possible conformations were limited by the observed position of residues 518–520 of the mTrxR2–NADP(H) structure. Although additional conformations are certainly possible given the highly mobile nature of this region of the protein (29), the model is consistent with several lines of biochemical evidence, as discussed below, and is a reasonable starting point for biochemical studies aimed at elucidating the precise mechanism of the enzyme. The eight-membered ring structure of the selenenylsulfide is juxtaposed to Cys-86 of the active-site disulfide/dithiol (Fig. 5). The

selenium atom of selenocysteine 523* is located nearly equidistant from the sulfur of Cys-86 and the epsilon nitrogen of His-497*. Similarly, the sulfur of Cys-522* is adjacent to the epsilon nitrogen of His-143. Last, the carboxylate of Gly-524* may interact with the positively charged side chain of Lys-506* (not shown).

Implications for Catalysis. The precise mechanism of selenenylsulfide/disulfide exchange has not yet been determined for mammalian TrxRs, but studies of *D. melanogaster* (DmTrxR1) (26, 48, 49) and *P. falciparum* (27, 37, 50) high- M_r TrxRs provide considerable insight. DmTrxR1 exhibits significant sequence homology to mammalian TrxRs but is not a selenoprotein (26, 48). It exhibits the salient features of catalysis described for selenocysteine-containing TrxRs but instead has a Ser-Cys-Cys-Ser motif at its C terminus. Bauer *et al.* (26) have identified Cys-57 and Cys-490* (equivalent to Cys-86 and Sec-523* in mTrxR2) as the two thiol groups involved in dithiol/disulfide exchange (26). Similarly, studies with *P. falciparum* TrxR have suggested that Cys 540* (comparable to Sec-523* in mTrxR2) is the C-terminal interchange thiol (27). The presented model of the C-terminal tail of mTrxR2 within the enzyme active site is consistent with Sec-523* interacting with active site dithiol/disulfide via Cys-86. After reduction of the selenenylsulfide, the resulting selenolate likely attacks the disulfide of oxidized thioredoxin (29), although this has not yet been experimentally confirmed.

This placement of the redox active C-terminal tail suggests several active-site residues that may facilitate catalysis (Fig. 5). An active-site glutamate–histidine pair is conserved in high- M_r TrxRs and is thought to promote reduction of the selenenylsulfide by stabilizing the resulting negative charge on the selenolate (28). Mutagenesis studies involving the analogous glutamate–histidine pair in *P. falciparum* TrxR have demonstrated that this histidine is required for efficient catalysis (27). In the mTrxR2 structure in which the C-terminal selenenylsulfide has been modeled (Fig. 5), the epsilon nitrogen of His 497* is located nearly equidistant from the sulfur of Cys-86 and the selenium of Sec-523* and is consistent with His-497* being involved in catalysis.

A second active-site histidine is observed in mTrxR2 that may contribute to catalysis. The epsilon nitrogen of His-143 is located ≈ 3 Å from the modeled sulfur of Cys-522*, and its imidazole ring appears to be oriented by an adjacent lysine residue, Lys-56 (Fig. 5). Interestingly, His-143 is replaced with a tyrosine residue in rTrxR1 (Tyr 116; Fig. 4B) and glutathione

reductase (Tyr-114). Site-directed mutagenesis studies in which Tyr-114 of glutathione reductase has been replaced with a leucine residue indicate that Tyr-114 is indeed involved in catalysis (47). The Y114L mutant exhibits a nearly 7-fold reduction in specific activity, and although not required for catalysis, Tyr-114 contributes to enzymatic efficiency. This observation, in concert with the proposed model, suggests that His-143 may be involved in the mechanism of mTrxR2. However, additional site-directed mutagenesis and kinetic studies will be required to assess the exact impact of His-143 on catalysis.

The thioredoxin-binding site of TrxR is thought to be located in the cleft between the FAD-binding domain and the dimer interface domain, near the C terminus of the enzyme (Figs. 1 and 2). In the absence of a high- M_r TrxR/thioredoxin complex structure, modeling studies have suggested interactions that mediate substrate recognition by TrxR (15, 28, 29). For rTrxR1, several amino acid side chains in the region comprised of residues 115–124 and the C-terminal tail were suggested to interact with thioredoxin (29). The corresponding regions in mTrxR2 (residues 142–151) have similar structural motifs but do exhibit some sequence variability. These differences may reflect different recognition residues on their respective thioredoxin substrates. However, without detailed structural information about the protein–protein complex, it remains difficult to ascribe function to particular residues.

Conclusion

Comparisons of mTrxR2 structures in the presence and absence of NADPH reveal several structural rearrangements that occur upon binding of the reduced pyridine nucleotide and suggest that an active-site tyrosine residue, Tyr-228, is essential for optimal placement of the nicotinamide ring of NADPH. Although mTrxR2 maintains the overall topology observed in cytosolic rat TrxR, several key active-site residues have been replaced. These substitutions probably impact enzymatic activity, but the importance of specific active-site residues to catalytic efficiency will need to be evaluated by site-directed mutagenesis and kinetic studies. In addition, a potential redox regulatory center has been identified that involves Cys-483 residues on opposing subunits. Collectively, these insights provided by examination of the reported crystal structures will assist in the design of further mechanistic studies of high- M_r TrxRs.

We thank Dr. Hideaki Moriyama and Dr. Kohei Homma of the University of Nebraska Structural Biology Core Facility for their contributions through the maintenance of the x-ray and computational resources, and Dr. Melanie A. Simpson (University of Nebraska) for thoughtful discussions regarding the manuscript. The project described was supported by National Institutes of Health Grants GM065204 (to V.N.G.) and P20 RR-17675 and by the Nebraska Research Initiative's funding of the Nebraska Center for Structural Biology.

- Holmgren, A. (1985) *Annu. Rev. Biochem.* **54**, 237–271.
- Gromer, S., Urig, S. & Becker, K. (2004) *Med. Res. Rev.* **24**, 40–89.
- Arner, E. S. & Holmgren, A. (2000) *Eur. J. Biochem.* **267**, 6102–6109.
- Williams, C. H., Arscott, L. D., Muller, S., Lennon, B. W., Ludwig, M. L., Wang, P. F., Veine, D. M., Becker, K. & Schirmer, R. H. (2000) *Eur. J. Biochem.* **267**, 6110–6117.
- Gromer, S., Wissing, J., Behne, D., Ashman, K., Schirmer, R. H., Flohe, L. & Becker, K. (1998) *Biochem. J.* **332**, 591–592.
- Novoselov, S. V. & Gladyshev, V. N. (2003) *Protein Sci.* **12**, 372–378.
- Williams, C. H., Jr. (1995) *FASEB J.* **9**, 1267–1276.
- Lennon, B. W., Williams, C. H., Jr., & Ludwig, M. L. (2000) *Science* **289**, 1190–1194.
- Muller, S., Gilberger, T. W., Farber, P. M., Becker, K., Schirmer, R. H. & Walter, R. D. (1996) *Mol. Biochem. Parasitol.* **80**, 215–219.
- Kanzok, S. M., Fechner, A., Bauer, H., Ulschmid, J. K., Muller, H. M., Botella-Munoz, J., Schneuwly, S., Schirmer, R. & Becker, K. (2001) *Science* **291**, 643–646.
- Gasdaska, P. Y., Gasdaska, J. R., Cochran, S. & Powis, G. (1995) *FEBS Lett.* **373**, 5–9.
- Gladyshev, V. N., Jeang, K. T. & Stadtman, T. C. (1996) *Proc. Natl. Acad. Sci. USA* **93**, 6146–6151.
- Gasdaska, P. Y., Berggren, M. M., Berry, M. J. & Powis, G. (1999) *FEBS Lett.* **442**, 105–111.
- Sun, Q. A., Wu, Y., Zappacosta, F., Jeang, K. T., Lee, B. J., Hatfield, D. L. & Gladyshev, V. N. (1999) *J. Biol. Chem.* **274**, 24522–24530.
- Sun, Q. A., Kirnarsky, L., Sherman, S. & Gladyshev, V. N. (2001) *Proc. Natl. Acad. Sci. USA* **98**, 3673–3678.
- Jakupoglu, C., Przemeczek, G. K., Schneider, M., Moreno, S. G., Mayr, N., Hatzopoulos, A. K., de Angelis, M. H., Wurst, W., Bornkamm, G. W., Brielmeier, M., et al. (2005) *Mol. Cell. Biol.* **25**, 1980–1988.
- Conrad, M., Jakupoglu, C., Moreno, S. G., Lippl, S., Banjac, A., Schneider, M., Beck, H., Hatzopoulos, A. K., Just, U., Sinowatz, F., et al. (2004) *Mol. Cell. Biol.* **24**, 9414–9423.
- Nalvarte, I., Damdimopoulos, A. E., Nystom, C., Nordman, T., Miranda-Vizuete, A., Olsson, J. M., Eriksson, L., Bjornstedt, M., Arner, E. S. & Spyrou, G. (2004) *J. Biol. Chem.* **279**, 54510–54517.
- Patenaude, A., Ven Murthy, M. R. & Mirault, M. E. (2004) *J. Biol. Chem.* **279**, 27302–27314.
- Sun, Q. A., Zappacosta, F., Factor, V. M., Wirth, P. J., Hatfield, D. L. & Gladyshev, V. N. (2001) *J. Biol. Chem.* **276**, 3106–3114.
- Damdimopoulos, A. E., Miranda-Vizuete, A., Treuter, E., Gustafsson, J. A. & Spyrou, G. (2004) *J. Biol. Chem.* **279**, 38721–38729.
- Miranda-Vizuete, A. & Spyrou, G. (2002) *Mol. Cells* **13**, 488–492.
- Rundlof, A. K., Janard, M., Miranda-Vizuete, A. & Arner, E. S. (2004) *Free Radic. Biol. Med.* **36**, 641–656.
- Su, D. & Gladyshev, V. N. (2004) *Biochemistry* **43**, 12177–12188.
- Arscott, L. D., Gromer, S., Schirmer, R. H., Becker, K. & Williams, C. H., Jr. (1997) *Proc. Natl. Acad. Sci. USA* **94**, 3621–3626.
- Bauer, H., Massey, V., Arscott, L. D., Schirmer, R. H., Ballou, D. P. & Williams, C. H., Jr. (2003) *J. Biol. Chem.* **278**, 33020–33028.
- Gilberger, T. W., Walter, R. D. & Muller, S. (1997) *J. Biol. Chem.* **272**, 29584–29589.
- Brandt, W. & Wessjohann, L. A. (2005) *ChemBioChem* **6**, 386–394.
- Sandalova, T., Zhong, L., Lindqvist, Y., Holmgren, A. & Schneider, G. (2001) *Proc. Natl. Acad. Sci. USA* **98**, 9533–9538.
- Mattevi, A., Obmolova, G., Sokatch, J. R., Betzel, C. & Hol, W. G. (1992) *Proteins* **13**, 336–351.
- Schulz, G. E., Schirmer, R. H., Sachsenheimer, W. & Pai, E. F. (1978) *Nature* **273**, 120–124.
- Zhang, Y., Bond, C. S., Bailey, S., Cunningham, M. L., Fairlamb, A. H. & Hunter, W. N. (1996) *Protein Sci.* **5**, 52–61.
- Bond, C. S., Zhang, Y., Berriman, M., Cunningham, M. L., Fairlamb, A. H. & Hunter, W. N. (1999) *Structure Fold. Des.* **7**, 81–89.
- Karplus, P. A. & Schulz, G. E. (1987) *J. Mol. Biol.* **195**, 701–729.
- Sarma, G. N., Savvides, S. N., Becker, K., Schirmer, M., Schirmer, R. H. & Karplus, P. A. (2003) *J. Mol. Biol.* **328**, 893–907.
- Zhong, L., Arner, E. S. & Holmgren, A. (2000) *Proc. Natl. Acad. Sci. USA* **97**, 5854–5859.
- Krnajski, Z., Gilberger, T. W., Walter, R. D. & Muller, S. (2000) *J. Biol. Chem.* **275**, 40874–40878.
- Pflugrath, J. W. (1999) *Acta Crystallogr. D* **55**, 1718–1725.
- Brunger, A. T., Adams, P. D., Clore, G. M., DeLano, W. L., Gros, P., Grosse-Kunstleve, R. W., Jiang, J. S., Kuszewski, J., Nilges, M., Pannu, N. S., et al. (1998) *Acta Crystallogr. D* **54**, 905–921.
- Jones, T. A., Zou, J. Y., Cowan, S. W. & Kjeldgaard. (1991) *Acta Crystallogr. A* **47**, 110–119.
- Lovell, S. C., Davis, I. W., Arendall, W. B., 3rd, de Bakker, P. I., Word, J. M., Prisant, M. G., Richardson, J. S. & Richardson, D. C. (2003) *Proteins* **50**, 437–450.
- Pettersen, E. F., Goddard, T. D., Huang, C. C., Couch, G. S., Greenblatt, D. M., Meng, E. C. & Ferrin, T. E. (2004) *J. Comput. Chem.* **25**, 1605–1612.
- Carugo, O., Cemazar, M., Zahariev, S., Hudaky, I., Gaspari, Z., Perczel, A. & Pongor, S. (2003) *Protein Eng.* **16**, 637–639.
- Xia, Z., Dai, W., Zhang, Y., White, S. A., Boyd, G. D. & Mathews, F. S. (1996) *J. Mol. Biol.* **259**, 480–501.
- Pai, E. F., Karplus, P. A. & Schulz, G. E. (1988) *Biochemistry* **27**, 4465–4474.
- Karplus, P. A. & Schulz, G. E. (1989) *J. Mol. Biol.* **210**, 163–180.
- Krauth-Siegel, R. L., Arscott, L. D., Schonleben-Janias, A., Schirmer, R. H. & Williams, C. H., Jr. (1998) *Biochemistry* **37**, 13968–13977.
- Gromer, S., Johansson, L., Bauer, H., Arscott, L. D., Rauch, S., Ballou, D. P., Williams, C. H., Jr., Schirmer, R. H. & Arner, E. S. (2003) *Proc. Natl. Acad. Sci. USA* **100**, 12618–12623.
- Jacob, J., Schirmer, R. H. & Gromer, S. (2005) *FEBS Lett.* **579**, 745–748.
- Wang, P. F., Arscott, L. D., Gilberger, T. W., Muller, S. & Williams, C. H., Jr. (1999) *Biochemistry* **38**, 3187–3196.